Carbohydrate Polymers 87 (2012) 1575–1582

Contents lists available at SciVerse ScienceDirect

Carbohydrate Polymers

journal homepage: www.elsevier.com/locate/carbpol

Microspheres based on mannosylated lysine-co-sodium alginate for macrophage-specific delivery of isoniazid

Sanjay Tiwari [a], Adya Prasad Chaturvedi [b], Yamini Bhusan Tripathi [b], Brahmeshwar Mishra [a,*]

[a] Department of Pharmaceutics, Institute of Technology, Banaras Hindu University, Varanasi 221005, Uttar Pradesh, India
[b] Department of Medicinal Chemistry, Institute of Medical Sciences, Banaras Hindu University, Varanasi 221005, Uttar Pradesh, India

ARTICLE INFO

Article history:
Received 9 July 2011
Received in revised form 3 September 2011
Accepted 22 September 2011
Available online 29 September 2011

Keywords:
Active targeting
Alveolar macrophages
Cell viability
Isoniazid
Spray drying

ABSTRACT

The present investigation reports coupling of ε- and α-amino groups of lysine (LS) with mannose (m-LS) and sodium alginate (SA), respectively, to reduce its toxicity. Prepared conjugate, m-LS-co-SA, was characterized through infra-red spectroscopy and differential scanning calorimetry. Cell viability studies were undertaken to assess the safety profile of the prepared conjugate. Microspheres, based on the conjugate, were prepared using spray drying technique and studied for targeting of isoniazid to alveolar macrophages (AMs). Pharmacokinetic studies of the optimized formulation batch were performed in Charles Foster rats.

Infra-red spectral data of the synthesized conjugate were in agreement to the presumptive sequence of the conjugation process. Dispersibility, thermal stability and safety of the conjugate were conducive to its biomedical application. Microspheres, formulated from the conjugate, were of uniform size and offered satisfactory drug loading efficiency and in vitro release characteristics. X-ray diffraction studies established that drug was entrapped within the microspheres rather than being adsorbed on to the surface. Pharmacokinetic studies revealed that the conjugate could be a potential vehicle towards both active targeting of isoniazid to AMs and controlling its release rate.

1. Introduction

Over the years, micro and nano-particulate carrier systems composed of poly-L-lysine (PLL) have widely been studied for the delivery of drugs and biomacromolecules. It displays unique property of binding to the cell membrane which is manifested as enhancement in its cellular uptake and transfection efficiency (Nounou et al., 2010; Takehara, Saimura, Inaba, & Hirohara, 2008). However, potential cytotoxicity associated with the high charge density and high molecular weight restricts the application of PLL as a drug carrier (Lanza et al., 1999; Nounou et al., 2010). Co-polymerization and derivatization with sugar molecules are the most widely studied approaches towards reducing the toxicity of PLL. Nounou et al. proposed low molecular weight (3.2 kDa) bioreducible co-polymer of L-lysine as an alternative to high molecular weight PLL. As compared to the control, a significant increase in transfection efficiency and reduction in cytotoxicity was achieved with the co-polymer (Nounou et al., 2010). Grosse, Tremeau-Bravard, Aron, Briand, and Fajac (2002) studied the intra-cellular trafficking of glycosylated PLL in cystic fibrosis airway epithelial cells. Carriers, coupled with sugar, resulted into higher localization of antibodies within lysosomes. There are other literature reports of the use of lower molecular weight fractions and co-administration with polyanions in the line of attempts to reduce the toxicity of PLL (Gonzalez Ferreiro, Tillman, Hardee, & Bodmeier, 2002; Majo, Alla, Bou, Herranz, & Munoz-Guerra, 2004; Nie et al., 2009).

Use of low molecular weight fraction and masking the amino groups constitute a potential strategy towards reducing the cytotoxicity of PLL (Derrien et al., 1989). Keeping this in our mind, in the present investigation, we tried multiple approaches to reduce the toxicity of lysine: (i) L-lysine, a low molecular weight fraction was used instead of PLL, (ii) ε-amino group was coupled with aldehyde group of mannose to form mannosylated lysine (m-LS), and (iii) α-amino group of m-LS was subjected to direct amidation with the carboxyl group of sodium alginate (SA) to from m-LS-co-SA. Coupling of mannose with the drug carriers has been a widely studied approach for macrophage specific delivery of various drugs (Liang, Shi, Deshpande, Malanga, & Rojanasakul, 1996; Vyas, Katare, Mishra, & Sihorkar, 2000). It helps in presentation of the carrier system to mannose specific membrane receptors and facilitates their preferential internalization (Yeeprae, Kawakami, Yamashita, & Hashida, 2006). Alginate is a water-dispersible, biocompatible and economical polysaccharide, composed of 1,4-linked β-D-mannuronate and 1,4-linked α-L-guluronate residues in varying proportions (Rees & Welsh, 1997). Conjugation of m-LS with SA would not only reduce its toxicity but would also modify

* Corresponding author.
E-mail address: bmishrabhu@rediffmail.com (B. Mishra).

0144-8617/$ – see front matter © 2011 Elsevier Ltd. All rights reserved.
doi:10.1016/j.carbpol.2011.09.056

the viscosity, improve drug loading efficiency and control the drug release rate from the carrier system (George & Abraham, 2006).

Inhalable microspheres based on m-LS-co-SA were prepared for macrophage specific delivery of isoniazid (INH) with the hypothesis that if a drug carrier, of respirable size distribution, enters via the same route as has been utilized by the mycobacteria, there would be an increased likelihood of co-localization of the carrier with pathogen and hence, increased therapeutic efficacy of drug could be anticipated (Gonzalez-Juarrero & O'Sullivan, 2011). Molecular interaction of sodium alginate and mannose was studied through infra-red spectroscopic studies. Thermal properties of the conjugate were studied through differential calorimetric analysis (DSC) and toxicity profile was assessed using 3-[4,5-dimethylthiazol-2-yl] 2,5-diphenyltetrazolium bromide (MTT) assay. Besides, microspheres prepared from the conjugate were subjected to in vitro and in vivo evaluations also.

2. Materials and methods

2.1. Materials

Isoniazid (INH) was received as a gift sample from Macleod Pharmaceuticals, Mumbai. Mannose, lysine hydrochloride, acetic acid and dimethyl sulfoxide (DMSO) were purchased from SD Fine Chemicals, Mumbai. Sodium alginate was purchased from Central Drug House, New Delhi. RPMI 1640, trichloroacetic acid (TCA) and 3-[4,5-dimethylthiazol-2-yl] 2,5-diphenyltetrazolium bromide (MTT) were purchased from Hi Media, Mumbai. Culture plates (96 well) were purchased from Tarsons Products Ltd., Kolkata. 1-Ethyl-3-(3-dimethylaminopropyl) carbodiimide (EDAC) was purchased from Sigma Aldrich, USA. Other solvents and chemicals were procured from manufacturers and were of analytical grade.

2.2. Animals

Male albino rats (Charles Foster strain; mean weight – 210 g) were procured from the Central Animal House, Banaras Hindu University. Animals were housed in plastic cages and maintained on a 12 h light/dark cycle at 21–25 °C and relative humidity of 45–55%. They were allowed free access to tap water and standard pelleted diet. All studies involving animals were conducted as per the procedures reviewed and approved by the Institutional Animal Ethical Committee of the Banaras Hindu University.

2.3. Preparation of mannosylated lysine and its coupling to sodium alginate

Lysine hydrochloride was activated by neutralization of its acid form with sodium hydroxide (Nounou et al., 2010). Equimolar quantity of activated lysine and mannose were allowed to react under mild magnetic stirring at room temperature (RT) for 24 h. Glacial acetic acid was used as catalyst. The reaction led to production of mannosylated lysine (m-LS) via Schiff base formation. Under this scheme, aldehyde group of mannose reacted with ε-amino group of lysine to form mannosylated lysine (m-LS). The product was purified by overnight dialysis (thickness – 0.025 mm, MWCO 6000–8000 Da) against distilled water and lyophilized to obtain an off-white powder.

Coupling of m-LS to SA was performed by the method described elsewhere (Novak, Banyai, Fleischer-Radu, & Borbely, 2007), with slight modifications. Carboxyl groups of aqueous dispersion of SA were first activated by EDAC and then, m-LS was added to it. The reaction was allowed to proceed for 48 h at room temperature under constant magnetic stirring. Formation of the conjugate (m-LS-co-SA) occurred through the reaction between α-amino group of m-LS and carboxylic acid group of sodium alginate. The product was subjected to two cycles of overnight dialysis against distilled water to remove unreacted reagents. Finally, it was frozen and lyophilized to obtain whitish, odorless and fibrous co-polymer, abbreviated as m-LS-co-SA.

2.4. Preparation of microspheres

Due to the advantages of being organic solvent-free and offering the possibility of easier scale up (Bodmeier, Chen, Tyle, & Jarosz, 1991), one-step spray-drying was used for the preparation of microspheres. Spray drying feedstock was prepared by dispersing INH in the aqueous dispersion of m-LS-co-SA. Spray drying was performed under the following experimental setting; feed concentration of 2.5% (w/v), inlet air temperature of 110 °C, outlet air temperature of 60 °C, pump setting of 12 rpm and 2 atm pressure. Spray dried microspheres were collected from the lower part of cyclone and the collecting vessel, stored in air-tight glass vials. They were subjected to various characterizations.

2.5. Characterizations

Conjugated polymer was characterized by Fourier transform infra-red spectroscopy (FT-IR). For FT-IR analysis, translucent pellet of each sample was prepared after grinding and dispersing it with KBr powder. It was then scanned over a wave number range of 400–4000 cm^{-1} by FT-IR spectrophotometer (Shimadzu, Model-8400, Japan). Data were collected over 40 scans at 4° resolution.

2.6. Evaluation of thermal properties of the synthesized conjugate

The thermal analysis of m-LS and m-LS-co-SA was performed using differential scanning calorimeter (DSC) (Mettler-Toledo STAR SW9.20, USA). Sample (~5 mg) was heated from 30 to 300 °C at the rate of 10 °C/min. Thermograms were acquired under the nitrogen flow of 10 ml/min. An empty aluminum pan was used as a reference.

2.7. Particle size and morphological characterizations

Particle size and size distribution of the microspheres were estimated by laser particle size analyzer, containing Helium–Neon laser of wavelength 632.8 nm and radiant power 5 mW (Akesmind 4800S, Japan). Shape and surface morphology were observed by field emission scanning electron microscope (S-4700, Hitachi, Japan). Prior to analysis, sample was mounted onto an aluminum stub and sputter-coated with platinum particles in argon atmosphere. Polydispersity index (PDI) and zeta potential of the microspheres were performed through a light scattering particle sizer (Beckman Coulter, Delsa^{TM} Nano, USA). Drug loading (%DL) of microspheres was calculated using the following formula:

$$\%DL = \frac{\text{Mass of INH loaded in microspheres}}{\text{Mass of INH loaded microspheres}} \times 100$$

2.8. X-ray diffraction studies

INH powder and optimized batch of prepared microspheres subjected to X-ray diffraction studies. They were conducted using powder X-ray diffractometer (Bruker D8, Germany). The sample was gently compressed into sample holder, and the powder surface was smoothed with a flat perspex block. Radiations scattered by sample in the crystalline region were recorded. X-ray spectra were acquired at room temperature in 2θ range of 20–70° in steps of 0.02° with scan rate of 2 steps/s. Besides, diffraction spectrum of the optimized formulation was utilized for its particle size

estimation using Debye–Scherrer equation (Burton, Ong, Rea, & Chan, 2009):

$$D_X = \frac{0.9\lambda}{B\cos\theta}$$

D_X is the diameter of microspheres (μm), λ is the X-ray wavelength (1.5414 Å in this case), 0.9 is Scherrer factor, B is the full width at half maxima and θ is Bragg angle.

2.9. In vitro drug release studies

In vitro drug release studies were performed as per the protocol described in our previous communication (Tiwari, Chaturvedi, Tripathi, & Mishra, 2011). MacIlvein buffer solution (MBS; pH 4) and phosphate buffer solution (PBS; pH 7.4) were independently used as release media. Formulation equivalent to 5 mg free drug was placed in the egg shell membrane, hermetically sealed and immersed into a 25 ml beaker containing 10 ml release media. It was maintained at 37 ± 0.5 °C and stirred at 50 rpm. Samples of 1 ml were collected at specific intervals and then topped up with the equivalent volume of pre-warmed fresh media. Each formulation was tested in triplicate and drug concentration was determined by UV spectrophotometer at a wavelength of 262 nm (Shimadzu 7800, Tokyo, Japan).

2.10. Cell viability assay

Cell viability was assessed by MTT colorimetric assay in 96-well culture plates using rat alveolar macrophages (AMs). Cells were harvested as described previously (Tiwari et al., 2011) and they were cultured at a seeding density of 1×10^5 cells/ml in RPMI 1640 supplemented with 10% foetal calf serum (FCS) and 1% antibiotics. LS, m-LS and m-LS-co-SA were individually dissolved in sterilized phosphate buffer solution (PBS) and their pH was adjusted to 6.8. In the case of m-LS-co-SA, a stock solution of 2% (w/v) was first prepared and thereafter, its dilutions were made up to the desired concentration(s). Cells were exposed to 100 μl of these solutions and incubated at 37 °C and 5% CO_2 for 18 h (Sanyo CO_2 Incubator, Japan). Following this, cells were subjected to treatment with 20 μl MTT (5 mg/ml in HEPES buffer) for 2 h (Florea, Thanou, Junginger, & Borchard, 2006). Plates were then centrifuged at 1500 rpm for 10 min (Remi C30, India), supernatant from each well was aspirated and the cell pellet was treated with 100 μl DMSO to assist cell lysis and dissolve formazon crystals. Its absorbance was measured at 590 nm using a microplate absorbance reader (Bio-Rad iMark™, USA). Cells treated with PBS acted as control. Cell viabilities were expressed as percentages relative to the result obtained with the control.

2.11. Assessment of uptake behavior of formulation by AMs

Qualitative uptake of the formulation (batch MS3) was assessed through fluorescence microscopy (Nikon, Japan). Microspheres (10 mg in 500 μl sterilized PBS), labeled with fluorescein sodium (FS), were administered to the rats through intra-tracheal instillation. Fluorescent labeling of microspheres was performed by adding 5 mg FS to 100 ml spray drying feed stock. At specific time point, AMs were harvested using a previously described procedure (Tiwari et al., 2011) and visualized at an excitation wavelength of 488 nm.

2.12. Pharmacokinetic studies

Animals were divided into two groups, each containing six animals ($n = 6$). Animals of group I were administered with 5 mg INH in 500 μl sterilized phosphate buffer saline through intra-tracheal instillation (Surti & Misra, 2008). Similarly, group II received formulation equivalent to 5 mg drug, dispersed in 500 μl PBS. At pre-specified time intervals ($t = 0$, 0.5, 1, 2, 4, 8, 16, 24 36 and 48 h), serial blood samples of approximately 200 μl were withdrawn from the retro-orbital plexus under mild ether anesthesia. Blood samples were cold centrifuged (10,000 rpm/10 min) and plasma was separated. Extraction of INH from plasma was performed with 10% trichloro acetic acid (TCA) and the extracted drug was analyzed by a well-validated HPLC procedure described previously (Tiwari et al., 2011).

Estimation of pharmacokinetic parameters was performed using Kinetica 5.0 (Trial Version). Maximum plasma concentration (C_{max}), time to achieve C_{max} (T_{max}) and mean residence time (MRT) were calculated. Area under plasma concentration–time curve $[AUC]_{0-48}$ was determined by trapezoidal method till last measurement point and was extrapolated to infinity $[AUC]_{0-\infty}$.

2.13. Statistical analysis

Each experiment was conducted in triplicate unless otherwise stated and the values were expressed as mean ± S.D. Comparison between the mean differences was performed by one-way ANOVA and p values of less than 0.05 were considered significant.

3. Results and discussion

3.1. FT-IR studies

Chemical characteristics of L-lysine favor its coupling to the mannose and SA. FT-IR spectra of lysine exhibited the characteristic absorption of primary amino group in the region 3300–3400 cm^{-1} (NH stretch) and 1600–1650 cm^{-1} (NH bend). m-LS showed shift of absorption peak to a lower wave number which was indicative of formation of –N=CH– bond (Fig. 1a and b). Upon coupling of m-LS with SA, peaks corresponding to carboxylate salt (1300–1420 cm^{-1}) were found to be diminished. This could be due to their carbodiimide assisted activation and conjugation with the amino group of m-LS to form amide linkage, appearing at 1614 cm^{-1}. Besides, shift of peak from higher (3300–3400 cm^{-1}) to lower wave number (3230–3300 cm^{-1}) and appearance of a strong peak at 3250 cm^{-1} were suggestive of formation of secondary amine from primary amine (Fig. 1c and d). It provided us an obvious evidence of successful amidation of carboxylic acid groups and covalent coupling of m-LS with SA.

3.2. Thermal properties of the synthesized conjugate

In case of m-LS, a relatively diffuse and broad endothermic dip could be detected in the region 40–45 °C which could be attributed to desorption of water molecules (Palomo, Ballesteros, & Frutos, 1999). Since the conjugation reaction was carried out in aqueous system, possibility of presence of water within the product could not be ruled out. A strong endothermic peak observed at 78 °C was indicative of temperature-induced phase transition and melting of the compound. Phase transition started at 66 °C and ended at 94 °C (Fig. 2a). On the other hand, m-LS-co-SA presented a broad endotherm which was shifted to a higher temperature region (180–220 °C). Broadening of peak in case of m-LS-co-SA could presumably be due to the chain relaxation characteristics imparted to the conjugate by SA (Fig. 2b). Besides, the prepared m-LS-co-SA was amorphous since no sharp melting temperature could be detected (Jha, Tiwari, & Mishra, 2011; Pang & Chu, 2010). Thus, DSC studies convinced us that thermal stability of m-LS was highly improved upon its conjugation with SA.

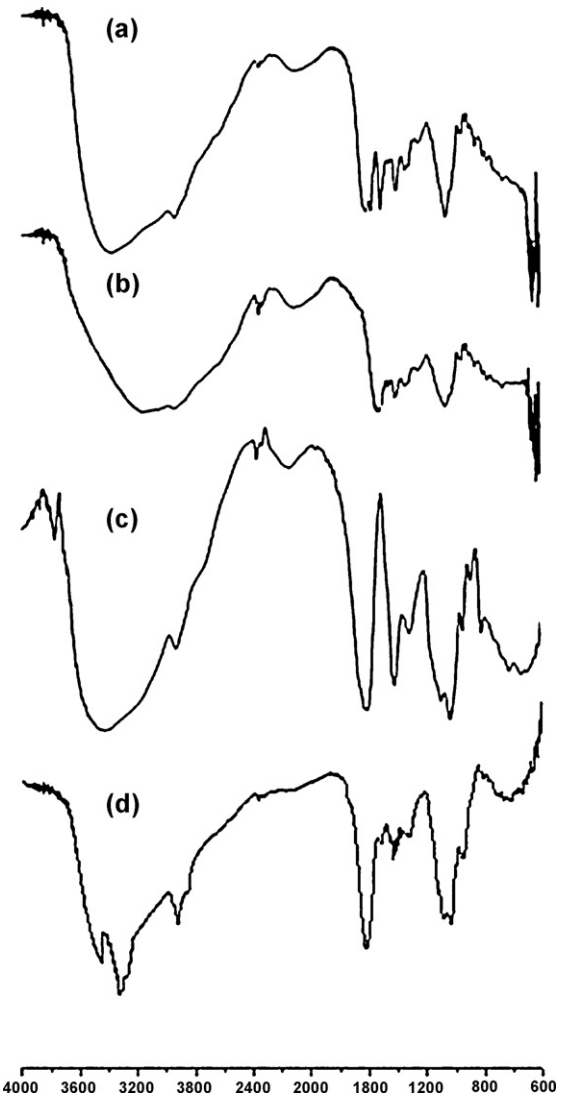

Fig. 1. FT-IR spectra of (a) LS, (b) m-LS, (c) SA and (d) m-LS-co-SA.

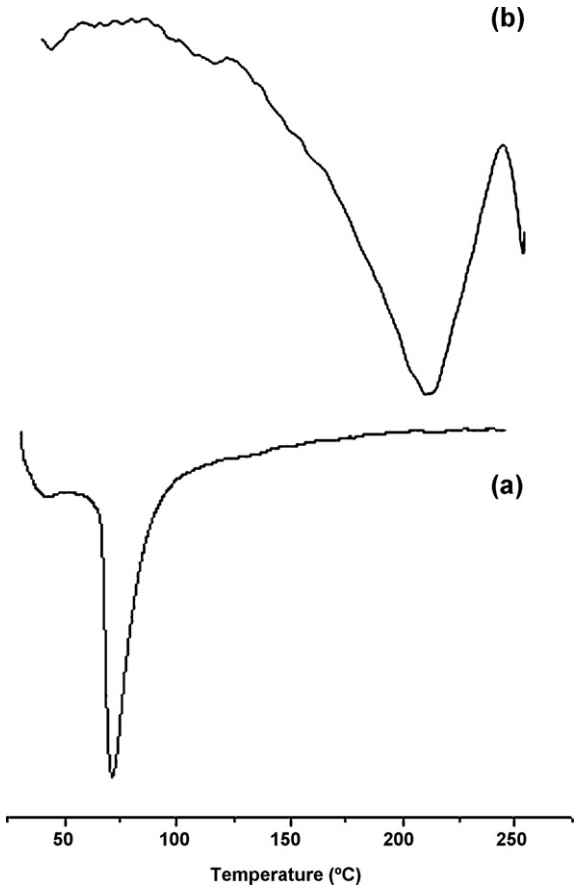

Fig. 2. Differential scanning calorimetric thermogram of (a) m-LS and (b) m-LS-co-SA.

3.3. Physicochemical characteristics of the prepared microspheres

Physicochemical characteristics of the spray-dried microspheres are presented in Table 1. Except for MS1, other batches provided yield ranging from 60 to 65% and no significant difference was noticed among them ($p < 0.05$). MS1 provided significantly lower yield (43%) which was resulted due to generation of more fraction of fines (Jha et al., 2011). It is likely that fine particles would have been blown away by cyclone. PDI value of batch MS4 was found to be significantly higher as compared to MS2 and MS3 ($p < 0.05$). With regard to zeta potential measurements, MS1 showed a significantly higher negative value which could possibly be due to its free amino groups. It is worth mentioning that zeta potential values of co-polymerized formulations (batches MS2, MS3 and MS4) shifted from higher negative value to lower negative value. These observations supported our hypothesis that amino groups were utilized during conjugation process and consequently, an upward shift in the zeta potential was observed. Drug loading of MS1 remained significantly lower in comparison to other formulations ($p < 0.05$) and this could have resulted owing to poor dispersion and matrix forming characteristics of m-LS. On the other hand, formulations composed of m-LS-co-SA (MS2, MS3 and MS4) showed an increase in loading efficiency which could possibly be due to their better matrix structure. Besides, as we increased the concentration of m-LS-co-SA from 0.5 to 2%, a significant increase in %DE was observed ($p < 0.05$). Though not to a significant extent, an increase in the mean size was also observed as we proceeded from MS1 to MS4. It could be attributed to the increment in viscosity of feedstock, which would have resulted into formation of larger droplets (Jha et al., 2011). Except for batch MS4, formulations from all the batches remained within respirable size range (Hirota et al., 2007).

3.4. SEM studies

As observed visually, m-LS did not show the tendency of film formation. SEM image of m-LS (Fig. 3a) were conducive to this observation. It exhibited poorly constituted strands with large and

Table 1
Physicochemical characteristics of the prepared microsphere formulations.

Batch code	Formulation composition (w/v)	Size, μm (±S.D.)	Polydispersity index (±S.D.)	Zeta potential (±S.D.)	Drug loading, % (±S.D.)
MS1	m-LS (1.5%)	0.54 ± 3.09	0.323 ± 0.261	−17.94 ± 2.18	17.58 ± 5.26
MS2	m-LS-co-SA (0.5%)	2.17 ± 3.68	0.189 ± 0.146	−3.92 ± 1.59	44.73 ± 7.05
MS3	m-LS-co-SA (1%)	3.54 ± 3.14	0.214 ± 0.139	−4.16 ± 1.18	70.16 ± 3.71
MS4	m-LS-co-SA (2%)	5.21 ± 7.85	0.562 ± 0.207	−3.21 ± 0.92	68.41 ± 4.30

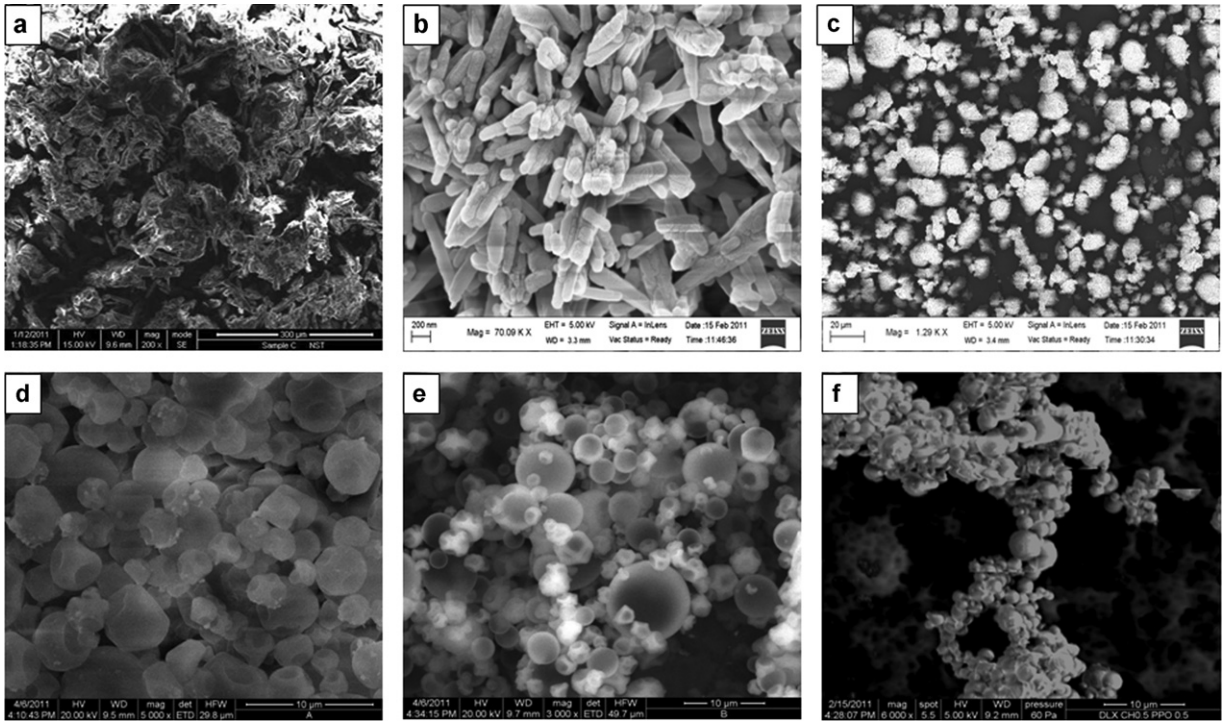

Fig. 3. Scanning electron microscopic image of (a) LS, (b) m-LS, (c) microspheres of batch MS1, (d) microspheres of batch MS2, (e) microspheres of batch MS3 and (f) microspheres of batch MS4.

widely placed non-spherical void spaces. The strands seemed to be apart and no interconnections could be observed. Similar characteristics were conceived by the microspheres composed of m-LS which possessed an irregular and deflated shape, with a granular outline (Fig. 3b). On the contrary, m-LS-co-SA showed distinct polymeric strands which were uniform in size and seemed to be arranged in a regular array. Nonetheless, the strands seemed to be interconnected throughout rather being isolated and no void spaces could be visualized (Fig. 3c). Such an arrangement rendered an efficient solute-solvent interaction and therefore, provided a better dispersion and fluid characteristics to the co-polymer. Accordingly, microspheres composed of m-LS-co-SA showed concentration dependent improvement in their surface profile and overall appearance. At a concentration of 0.5%, w/v (batch MS2), microspheres with a corrugated surface were produced. Prominent invaginations could be clearly visualized on their surface (Fig. 3d). Increasing its concentration to 1% (w/v) resulted into particles with rounded appearance and even surface profile (Fig. 3e). However, microspheres from batch MS4 exhibited considerable aggregation which could be attributed to the increased viscosity of the polymeric dispersion (Fig. 3f). SEM results signified that covalent coupling between m-LS and SA would have resulted into formation of cohesive strands which not only provided an even coverage of particle surface but also acted as a mechanical barrier thus restricting their coalescence and formation of discrete particles.

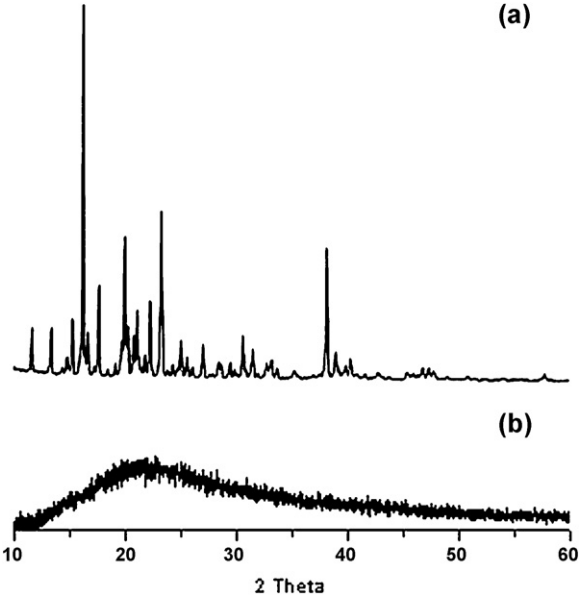

Fig. 4. X-ray diffraction spectra of (a) pure INH and (b) batch MS3.

3.5. X-ray diffraction studies

X-RD studies were performed to verify the incorporation of drug within the microspheres. Diffraction spectrum of drug sample showed distinct and high intensity peaks in the region of 2θ ranging from 15° to 25° (Fig. 4a). However, in case of drug-loaded microspheres (batch MS3), no such peaks could be observed (Fig. 4b). This could have occurred due to entrapment of drug within the microspheres (Jha et al., 2011). From these observations, we concluded that the drug was efficiently loaded within the microspheres and the amount of surface-adsorbed drug could be considered as negligible. Particle size of optimized batch of microspheres, as estimated by X-RD studies, was found to be 2.91 μm, which agreed well to the observations with laser particle size analyzer.

3.6. In vitro drug release studies

Formulations exhibited characteristic difference in their release profiles depending upon their respective compositions (Fig. 5). Batches MS1 and MS2 provided high initial burst release. Within

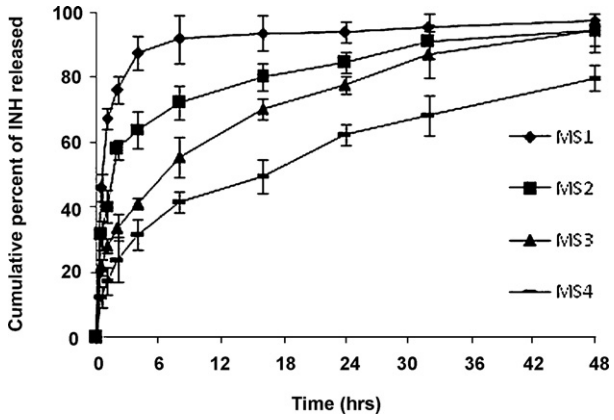

Fig. 5. In vitro release of INH from the prepared microspheres (bars represent ±standard deviation; $n = 3$).

first 60 min, MS1 and MS2 provided a cumulative drug release of 67% and 40%, respectively. Besides, it is worth mentioning that virtually no drug release was observed from MS1 after 8 h. It could possibly be due to poor matrix structure constituted by MS1 which could not control the drug diffusion in response to higher concentration gradient generated initially. Considering these aspects, MS3 and MS4 offered significantly different release characteristics ($p < 0.05$; one way ANOVA).

We observed a sustained release profile of INH from MS3 and MS4 even during initial phase. This illustrates that covalent structure constituted by m-LS-co-SA afforded a tightly packed matrix which was less porous and underwent controlled swelling. It, therefore, entrapped the drug more effectively and hindered its diffusion across the microsphere matrix. These effects, taken together, were evidently realized as controlled release profile of INH lasting up to 48 h. In comparison to the other batches, a significant decrease in the rate and extent of drug release was observed with MS4; only 80% drug release occurred from it at the end of 48 h ($p < 0.05$). These results tend to prove that a sustained release of INH can be obtained by incorporating it into m-LS-co-SA microspheres. Further, no significant difference was observed in the release rate of MS3 and MS4 in MacIlvein buffer solution (MBS; pH 4) and phosphate buffer solution (PBS; pH 7.4).

Batch MS3 provided the microspheres with better morphological features, respirable size range, satisfactory drug loading and in vitro drug release characteristics. Therefore, its composition was considered to be optimized and it was used for performing the formulation uptake studies in AMs and pharmacokinetic studies in animals.

3.7. Cell viability assay

The results of cell viability assay showed that after 18 h incubation with LS, only 24.28% of cells remained viable. Studies were conducted at pH 6.8, which favored the activation of LS (Nounou et al., 2010) and this, in turn, increased its binding affinity to the cells. This was manifested as its potential toxicity to the cells. However, a significant difference in cellular viability was observed between native and derivatized LS ($p < 0.05$). For example, a remarkable increase in viability was observed in the cells treated with m-LS. This improvement could possibly have been resulted subsequent to the masking of ε-amino group of LS. Further, no significant cytotoxic effects, relative to control, were observed in the cells during the period of incubation even when they were exposed to m-LS-co-SA at concentration as high as 10 mg/ml. Cells treated with 20 mg/ml m-LS-co-SA demonstrated lower viability as compared to its lower concentrations. However, this effect remained insignificant ($p > 0.05$) and it could be attributed to the higher viscosity of the polymer (Florea et al., 2006).

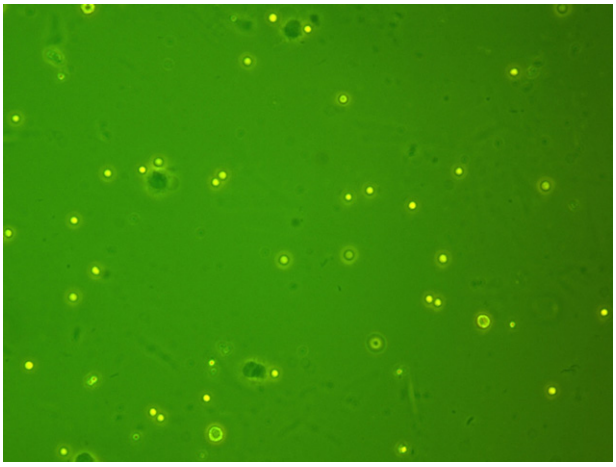

Fig. 6. Fluorescent micrograph of the microspheres engulfed within alveolar macrophages.

Since test compounds were structurally related, each of them contained identical monomer content and experimental conditions were kept constant throughout, the number of primary amino groups could be the sole decisive factor affecting the survival of cells. This study demonstrated that derivatization of primary amino groups resulted significant reduction in the cytotoxicity of lysine. It corroborated to the findings of Dutta, Garg, and Jain (2008) who reported a reduction in the cytotoxicity of a cationic dendrimer through its conjugation with tuftsin.

3.8. Assessment of uptake behavior of formulation by AMs

As can be visualized through the fluorescent micrographs, microsphere formulations appeared to be intracellular or even nuclear. Within 15 min of administration of the formulation, strong intracellular fluorescence was observed in the cytosol of AMs (Fig. 6). This was indicative that endocytosis took place effectively. Translating this prompt internalization and distribution behavior of the formulation in terms of its therapeutic effectiveness, the carrier system could be proposed to be more interesting since more amount of drug could be internalized within the AMs which constitute the desired site of action for anti-tubercular drugs. Such treatment modality is expected to avoid the chances of microbial persistence and recurrent infections.

3.9. Pharmacokinetic studies

Pharmacokinetic parameters of INH were estimated following intra-tracheal administration of batch MS3. The efficacy of microsphere formulation relative to drug solution was established in terms of AUC, C_{max}, T_{max}, MRT and $AUC_{0-\infty}$. As can be seen from the mean plasma concentration–time curve (Fig. 7), INH solution resulted into faster appearance of drug in plasma which agrees well to our previous finding (Tiwari et al., 2011). Microspheres, on the other hand, displayed entirely different pharmacokinetics. Plasma level of INH during absorption phase remained significantly lower to that of drug solution which could have been due to uptake of formulation by AMs during initial phase. Presence of a mannose terminal within the carrier system would have a synergistic effect to the uptake process (Chono, Tanino, Seki, & Morimoto, 2008). Once the uptake capacity of macrophages was surpassingly overwhelmed, a steady increase in plasma concentration of drug was observed.

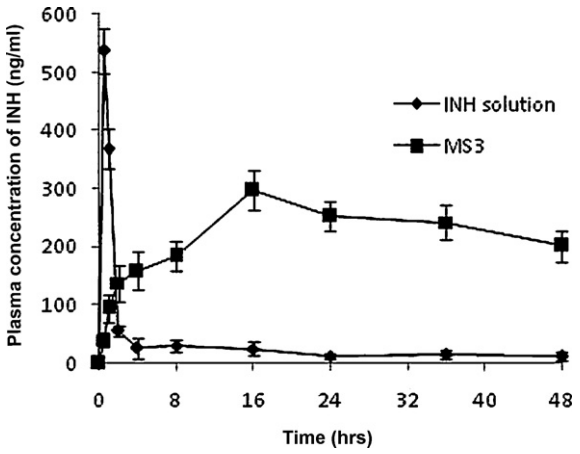

Fig. 7. Plasma concentration vs. time profiles of microspheres (batch MS3) and pure drug solution following intra-tracheal instillation to rats (bars represent ±standard deviation; $n = 6$).

A significant increase in the T_{max} of INH was noticed with the microspheres formulations ($p < 0.01$). Microspheres provided a steady plasma concentration profile of INH and the drug concentration was maintained without appearance of peaks and valleys. MRT of drug was significantly prolonged ($p < 0.01$). Approximately eight fold increment was observed in the value of $AUC_{0-\infty}$. The increase in AUC and MRT and decrease in C_{max} reflect that microsphere formulations could reduce the toxic complications arising out of fluctuations in the plasma level of drug. These observations coupled with fluorescence microscopic studies were suggestive that the delivery system not only targeted the AMs but also resulted into prolonged presence of drug in the blood. Targeting ability of the formulation would inhibit the intracellular multiplication of the pathogen whereas maintenance of plasma drug concentration within therapeutic window would help in eliminating the microbial load from the other infected tissues.

4. Conclusions

In the present work, we have reported successful preparation of m-LS-co-SA conjugate following a mild and simple reaction procedure. FT-IR spectral data of the prepared conjugate were in agreement to the presumptive pathway of reaction. The conjugate presented good dispersibility in water and an improved thermal stability profile. In vitro cytotoxicity results showed that m-LS-co-SA has no significant toxic effects up to a concentration as high as 20 mg/ml and it could be used for macrophage specific delivery of INH. Microspheres formulated from the conjugate provided satisfactory loading efficiency and drug release characteristics. X-RD studies established that drug was entrapped within the microspheres rather than being adsorbed on to the surface. They offered respirable size range and possessed a uniform size distribution. Preliminary studies underscored that the conjugate can have multifaceted applications in the active targeting strategies, especially for the diseases mediated by macrophages. However, further studies are warranted to investigate the toxicity and biodegradation aspects of conjugate as different set of cells can differ in their biological response towards the proposed carrier.

Conflict of interest

The authors report no conflicts of interest. The authors alone are responsible for the content and writing of the paper.

Acknowledgements

First author acknowledges the financial assistance of Council of Scientific and Industrial Research, New Delhi, in carrying out this research work. The support of Prof. O.N. Srivastava and Dr. R.K. Singh (Department of Physics, Banaras Hindu University) is thankfully acknowledged for providing the facility of SEM and DSC studies, respectively. Sincere thanks go to Prof. P.K. Jha (Department of Physics, Bhavnagar University, Gujarat) for carefully carrying out X-RD studies.

References

Bodmeier, R., Chen, H., Tyle, P. & Jarosz, P. (1991). Pseudophedrine HCl microspheres formulated into an oral suspension dosage form. *Journal of Controlled Release*, *15*, 65–77.

Burton, A. W., Ong, K., Rea, T. & Chan, I. Y. (2009). On the estimation of average crystallite size of zeolites from the Scherrer equation: A critical evaluation of its application to zeolites with one-dimensional pore systems. *Microporous and Mesoporous Materials*, *117*, 75–90.

Chono, S., Tanino, T., Seki, T. & Morimoto, K. (2008). Efficient drug targeting to rat alveolar macrophages by pulmonary administration of ciprofloxacin incorporated into mannosylated liposomes for treatment of respiratory intracellular parasitic infections. *Journal of Controlled Release*, *127*, 50–58.

Derrien, D., Midoux, P., Petit, C., Negre, E., Mayer, R., Monsigny, M., et al. (1989). Muramyl dipeptide bound to poly-L-lysine substituted with mannose and gluconoyl residues as macrophage activators. *Glycoconjugate Journal*, *6*, 241–255.

Dutta, T., Garg, M. & Jain, N. K. (2008). Targeting of efavirenz loaded tuftsin conjugated poly(propyleneimine) dendrimers to HIV infected macrophages *in vitro*. *European Journal of Pharmaceutical Sciences*, *34*, 181–189.

Florea, B. I., Thanou, M., Junginger, H. E. & Borchard, G. (2006). Enhancement of bronchial octreotide absorption by chitosan and N-trimethyl chitosan shows linear in vitro/in vivo correlation. *Journal of Controlled Release*, *110*, 353–361.

George, M. & Abraham, T. E. (2006). Polyionic hydrocolloids for the intestinal delivery of protein drugs: Alginate and chitosan—A review. *Journal of Controlled Release*, *114*, 1–14.

Gonzalez Ferreiro, M., Tillman, L., Hardee, G. & Bodmeier, R. (2002). Characterization of alginate/poly-L-lysine particles as antisense oligonucleotide carriers. *International Journal of Pharmaceutics*, *239*, 47–59.

Gonzalez-Juarrero, M. & O'Sullivan, M. P. (2011). Optimization of inhaled therapies for tuberculosis: The role of macrophages and dendritic cells. *Tuberculosis*, *91*, 86–92.

Grosse, S., Tremeau-Bravard, A., Aron, Y., Briand, P. & Fajac, I. (2002). Intracellular rate-limiting steps of gene transfer using glycosylated polylysines in cystic fibrosis airway epithelial cells. *Gene Therapy*, *9*, 1000–1007.

Hirota, K., Hasegawa, T., Hinata, H., Ito, F., Inagawa, H., Kochi, C., et al. (2007). Optimum conditions for efficient phagocytosis of rifampicin-loaded PLGA microspheres by alveolar macrophages. *Journal of Controlled Release*, *119*, 69–76.

Jha, R. K., Tiwari, S. & Mishra, B. (2011). Bioadhesive microspheres for bioavailability enhancement of raloxifene hydrochloride: Formulation and pharmacokinetic evaluation. *AAPS PharmSciTech*, *12*, 650–657.

Lanza, R. P., Jackson, R., Sullivan, A., Ringeling, J., Mc-Grath, C., Kuhtreiber, W., et al. (1999). Xenotransplantation of cells using biodegradable microcapsules. *Transplantation*, *67*, 1105–1111.

Liang, W. W., Shi, X., Deshpande, D., Malanga, C. J. & Rojanasakul, Y. (1996). Oligonucleotide targeting to alveolar macrophages by mannose receptor-mediated endocytosis. *Biochimica Biophyscia Acta*, *1279*, 227–234.

Majo, M. A., Alla, A., Bou, J. J., Herranz, C. & Munoz-Guerra, S. (2004). Synthesis and characterization of polyamides obtained from tartaric acid and L-lysine. *European Polymer Journal*, *40*, 2699–2708.

Nie, H., Khew, S. K., Lee, L. Y., Poh, K. L., Tong, Y. W. & Wang, C. H. (2009). Lysine-based peptide-functionalized PLGA foams for controlled DNA delivery. *Journal of Controlled Release*, *138*, 64–70.

Nounou, M. I., Emmanouil, E., Chung, S., Pham, T., Lu, Z. & Bikram, M. (2010). Novel reducible linear L-lysine-modified copolymers as efficient nonviral vectors. *Journal of Controlled Release*, *143*, 326–334.

Novak, L., Banyai, I., Fleischer-Radu, J. E. & Borbely, J. (2007). Direct amidation of poly(γ-glutamic acid) with benzylamine in dimethyl sulfoxide. *Biomacromolecules*, *8*, 1624–1632.

Palomo, M. E., Ballesteros, M. P. & Frutos, P. (1999). Analysis of diclofenac sodium and derivatives. *Journal of Pharmacy and Biomedical Analysis*, *21*, 83–94.

Pang, X. & Chu, C. C. (2010). Synthesis characterization and biodegradation of functionalized amino acid-based poly(ester amide)s. *Biomaterials*, *31*, 3745–3754.

Rees, D. A. & Welsh, E. J. (1997). Secondary and tertiary structure of polysaccharides in solutions and gels. *Angewandte Chemie International Edition*, *16*, 214–224.

Surti, N. & Misra, A. N. (2008). Wheat germ agglutinin-conjugated nanoparticles for sustained cellular and lung delivery of budesonide. *Drug Delivery*, *15*, 81–86.

Takehara, M., Saimura, M., Inaba, H. & Hirohara, H. (2008). Poly(-L-diaminobutanoic acid), a novel poly(amino acid), coproduced with poly(-L-lysine) by two strains of Streptomyces celluloflavus. *FEMS Microbiology Letters*, *286*, 110–117.

Tiwari, S., Chaturvedi, A. P., Tripathi, Y. B. & Mishra, B. (2011). Macrophage specific targeting of isoniazid through mannosylated gelatin microspheres. *AAPS PharmSciTech*, *12*, 900–908.

Vyas, S. P., Katare, Y. K., Mishra, V. & Sihorkar, V. (2000). Ligand directed macrophage targeting of amphotericin B loaded liposomes. *International Journal of Pharmaceutics*, *210*, 1–14.

Yeeprae, W., Kawakami, S., Yamashita, F. & Hashida, M. (2006). Effect of mannose density on mannose receptor-mediated cellular uptake of mannosylated o/w emulsions by macrophages. *Journal of Controlled Release*, *114*, 193–201.